ChemPubSoc Europe

DOI: 10.1002/cctc.201501021

CHEMCATCHEM Full Papers

Ruthenium and Formic Acid Based Tandem Catalytic Transformation of Bioderived Furans to Levulinic Acid and Diketones in Water

Ambikesh D. Dwivedi,[a] Kavita Gupta,[a] Deepika Tyagi,[a] Rohit K. Rai,[a] Shaikh M. Mobin,[a] and Sanjay K. Singh*[a, b]

Efficient tandem catalytic transformations of bioderived furans, such as furfural, 5-hydroxymethylfurfural (5-HMF), and 5-methylfurfural (5-MF), to levulinic acid (LA) and diketones, 1-hydroxyhexane-2,5-dione (1-HHD), 3-hydroxyhexane-2,5-dione (3-HHD), and hexane-2,5-dione (2,5-HD), was achieved by using water-soluble arene–Ru^{II} complexes, containing ethylenediamine-based ligands, as catalysts in the presence of formic acid. The catalytic conversion of furans depends on the catalyst, ligand, formic acid concentration, reaction temperature, and time. Experimental evidence, including time-resolved ^{1}H NMR spectral studies, indicate that the catalytic reaction proceeds first with formyl hydrogenation followed by hydrolytic ring opening of furans. The ruthenium–formic acid tandem catalytic transformation of fructose to diketones and LA was also achieved. Finally, the molecular structures of the four representative arene–Ru^{II} catalysts were established by single-crystal X-ray diffraction studies.

Introduction

Development of new methodologies for biomass transformation is gaining extensive attention. As biomass, a viable resource of carbon and extensively dispersed in nature, has shown its potential for the production of carbon-based energy sources and several valuable platform chemicals, it can probably replace or provide an alternative to the currently used fossil fuel and fine chemicals.[1] As direct usage of biomass is not sustainable to date, the transformation of carbohydrates (monosaccharides or disaccharides)[2–4] or bioderived furans (such as 5-hydroxymethylfurfural (5-HMF) or furfural)[5] to fuel components or chemicals has been extensively studied in recent years, as these are regarded as the key components of biomass. In particular, the furans (5-HMF or furfural) have received considerable attention for transformation to several valuable chemicals and biofuel, possibly owing to the inherent structural patterns available in these furans.[5–7] Several chemical processes such as hydrogenation and/or hydrolysis direct transformations of furans to important chemicals such as levulinic acid (LA), succinic acid, diketones, furfuryl alcohol, 2,5-dimethyl furan, 2,5-bis(hydroxymethyl)furan, pentane-2,5-diol, and others,[5,6] whereas furan carboxylic acids can be obtained by selective oxidation of formyl groups of furfural and its derivatives.[7] Complete hydrogenation and hydrolytic ring opening of furans and its aldol adducts with extended carbon chains, obtained by aldol condensation of furfural or its derivatives with acetone, may produce C5–C9 alkanes for direct application as fuel.[8] Moreover, one of the diketone products, 3-hydroxyhexane-2,5-dione (3-HHD), also known as Henze's ketol, obtained during the catalytic transformation of 5-methylfurfural (5-MF), is known for its significant biological activity and was also identified in plant extracts.[9] Ketoacids and diketones obtained from the catalytic transformation of furans have been extensively used as platform chemicals for the production of several important fine chemicals (e.g., esters, alcohols, lactones, amines, and cycloketones) or biofuel components such as blenders for gasoline.[10] Particularly, ketoacid (LA) has been identified by the US Department of Energy (DOE) as one of the important target chemicals in their biomass program.[11] Some of the key features, such as the presence of a carbonyl group, carboxylic group, and an α-H present in LA, have resulted in its usage as an important key starting material in several important reactions for industrial applications (Scheme 1).[12] Some of the very important end products obtained from LA are calcium levulinate (a new supplement for calcium), 5-aminolevulinic acid (used for photodynamic therapy (PDT) of tumor-like human meningioma, and a biodegradable herbicide), γ-valerolactone (GVL), and 2-methyltetrahydrofuran (used as a fuel blender), and so on.

Several new and diverse catalytic processes for the selective transformation of furan derivatives into open-ring components are being explored, particularly, by using heterogeneous catalysts.[5–7,13–15] For instance, Au nanoparticles were reported for the direct conversion of 5-HMF to the corresponding diketones by hydrogenation/hydrolytic ring opening in the presence of

[a] A. D. Dwivedi, K. Gupta, D. Tyagi, R. K. Rai, Dr. S. M. Mobin, Dr. S. K. Singh
Discipline of Chemistry, School of Basic Sciences
Indian Institute of Technology (IIT) Indore
Indore 452 017, Madhya Pradesh (India)

[b] Dr. S. K. Singh
Centre for Material Science and Engineering
Indian Institute of Technology (IIT) Indore
Indore 452 017, Madhya Pradesh (India)

Supporting information for this article is available on the WWW under http://dx.doi.org/10.1002/cctc.201501021.

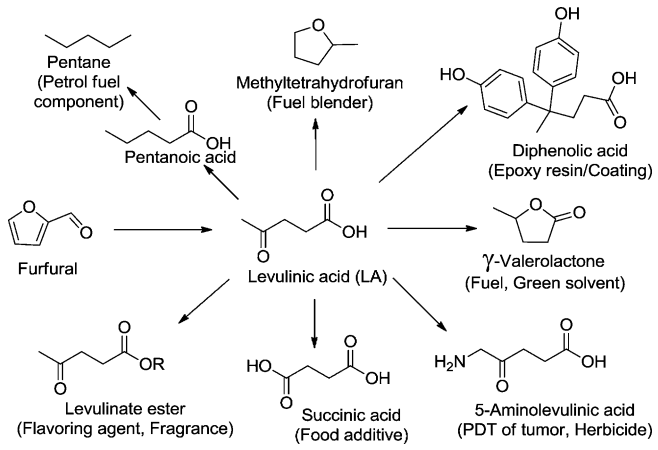

Scheme 1. Selected applications of levulinic acid.

H_3PO_4.[14] In the same direction, Pd/C-based catalysis has also been reported for similar transformations of 5-HMF/furfural to diketones and ketoacids by using CO_2/H_2O (120 °C) or Amberlyst 70 (170 °C).[15] However, homogenous catalysts for this class of reactions are seldom reported. Zhang et al. reported Cp*–iridium complexes (Cp* = pentamethylcyclopentadiene) catalyzed the conversion of furans to ketones under 20 bar of H_2 gas at 110 °C. The reaction proceeded with initial catalytic hydrogenation of 5-HMF followed by a ring-opening reaction facilitated by in situ generated acid.[16] Recently, we also explored the catalytic efficacy of 8-aminoquinoline-coordinated arene–ruthenium(II) catalyst for the transformation of furans to LA and diketones.[17]

Arene–Ru^{II} complexes, such as ethylenediamine-based ruthenium complexes or Shvo's catalyst, represent a well-established class of active catalysts for efficient hydrogenation of carbonyl groups in ketones, aldehydes, esters, C=N bonds in imines, or C=C bonds in styrene or furfuryl alcohol.[18] The excellent synergistic cooperation between the metal and ligand in these complexes, such as the availability of N–H bonds to facilitate transfer hydrogenation reactions, accounts for the high catalytic performances of the complexes in hydrogenation reactions using H_2 or other H-donors, for example, formic acid.[18,19] These insights encouraged us to employ the arene–Ru^{II} complexes containing simple ethylenediamine-based ligands in the highly efficient transformation of bioderived furans to open-ring components. Moreover, using formic acid not only satisfies the requirement of a H-donor but also provides plenty of H^+ ions. However, it is worth mentioning here that using excess acid may lead to humin formation from furan derivatives.[20] Furthermore, the high aqueous solubility and stability displayed by most of the arene–Ru^{II} complexes may offer easy recovery and reuse of the catalyst. Although literature reports highlight the competence of several ruthenium complexes for hydrogenation of furfural and 5-hydroxymethylfurfural (5-HMF) to the corresponding alcohols (furfuryl alcohol and 2,5-bis(hydroxymethyl)furan),[21] employing arene–Ru^{II} complexes with formic acid for tandem catalytic transformation of furans is rarely explored.[17] Therefore, to enrich and enhance the understanding about the ruthenium-catalyst-based transformation of furans, the development of new highly active and water-soluble catalytic systems are highly required.

In our continuous efforts in this direction, we report here the use of highly water soluble arene–Ru^{II} complexes containing simple ethylenediamine-based ligands for the tandem catalytic transformation of bioderived furans to open-ring components (ketoacids and diketones), in water under moderate reaction conditions. A structure–activity relationship in terms of N–H bond availability was also explored. An important reaction intermediate, furfuryl alcohol, was identified by ^{1}H NMR spectroscopy, which provided additional insights into the mechanism of the catalytic transformation of furfural to LA, and also the role of the ruthenium catalyst and the formic acid. Moreover, the biomass feedstock of furans, fructose, was also catalytically transformed to diketones with limited conversion. Herein, we also report the X-ray structural characterization of the representative arene–Ru^{II} complexes employed for the catalytic reactions.

Results and discussion

Syntheses and characterization of arene–Ru^{II} catalysts

Cationic monometallic arene–Ru^{II} complexes (**[Ru]-1**–**[Ru]-8**) containing ethylenediamine ligand or its derivatives were synthesized by treating the dichloro-bridged arene–Ru^{II} dimer with the appropriate bidentate ethylenediamine-based ligand in methanol at room temperature.[22] The identities of the synthesized complexes were established by NMR spectroscopy, elemental analysis, and ESI mass spectrometry, and the results corroborated well with the proposed formula of the complexes as $[(\eta^6\text{-arene})RuCl(\kappa^2L)]^+$ (where η^6-arene = C_6H_6 or $C_{10}H_{14}$, and L = $H_2NCH_2CH_2NH_2$ (en), $H_2NCH_2CH_2NH(CH_3)$ (Me_1en), $H_2NCH_2CH_2N(CH_3)_2$ (Me_2en), or $(CH_3)HNCH_2CH_2N(CH_3)_2$ (Me_3en) (Figure 1). Suitable crystals of arene–Ru^{II} complexes **[Ru]-2**, **[Ru]-6**, **[Ru]-7**, and **[Ru]-8** were grown by slow evaporation of the methanol/dichloromethane solution of the respective complexes. The crystals were subjected to single-crystal X-ray diffraction analysis to confirm the structures as $[(\eta^6\text{-}C_6H_6)RuCl(Me_1en)]PF_6$ (**[Ru]-2**), $[(\eta^6\text{-}C_{10}H_{14})RuCl(Me_1en)]PF_6$ (**[Ru]-6**), $[(\eta^6\text{-}C_{10}H_{14})RuCl(Me_2en)]PF_6$ (**[Ru]-7**), and $[(\eta^6\text{-}C_{10}H_{14})RuCl(Me_3en)]PF_6$ (**[Ru]-8**) (Figure 1 and Tables S1–S2 in the Supporting Information).

All the complexes display analogous molecular structures with the characteristic piano-stool geometry of arene–Ru^{II} complexes, with the η^6-coordinated arene ring as the top and the two nitrogen atoms of the respective ethylenediamine-based ligand and one chloride ligand as the three legs. The complexes **[Ru]-2**, **[Ru]-7**, and **[Ru]-8** crystallize in the monoclinic $P2_1$ space group, whereas the complex **[Ru]-6** is in the triclinic $P\bar{1}$ space group. The arene ring (η^6-benzene or η^6-*p*-cymene) appears almost planar for all the complexes; the centroid of the arene ring is displaced by 1.65–1.69 Å from the Ru^{II} center. The Ru–nitrogen and Ru–chloride bond lengths are within the ranges 2.11–2.19 Å and 2.40–2.42 Å, respectively, which are close to those reported previously for related arene–Ru^{II} com-

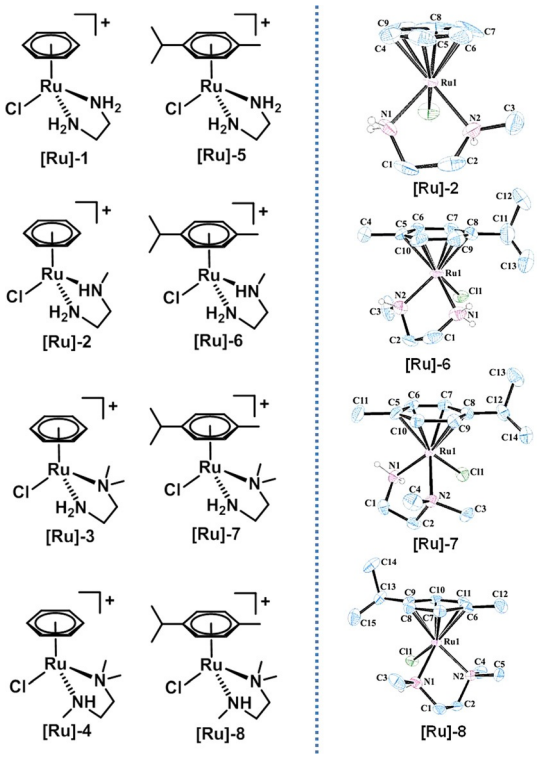

Figure 1. Schematic representation of the arene–Ru^{II} catalysts **[Ru]-1**–**[Ru]-8** (left), and the X-ray crystal structures of the representative catalysts **[Ru]-2**, **[Ru]-6**, **[Ru]-7**, and **[Ru]-8** (right; thermal ellipsoids drawn at the 30% probability level) used for water-based catalytic transformation of furanic compounds. Counter anions, PF_6, and hydrogen atoms (except those on nitrogen atoms) are omitted for clarity.

plexes.[22,23] Moreover, the Cl–Ru–N and N–Ru–N bond angle ranges are 82.4–88.1° and 78.3–79.8°, respectively, and those between the legs and the centroid of the η^6-arene ring is 124.5–133.8°; the observed values are comparable with those reported for other analogous complexes.[22,23]

Catalytic transformation of furan derivatives

The catalytic efficacy of the water-soluble catalysts **[Ru]-1**–**[Ru]-8** was explored for the aqueous-phase tandem transformation of furan derivatives into LA and diketones. Readily available furan derivative, furfural (**1a**), was selected as the model substrate for the catalytic reaction. In the first set of experiments, the influence of the additive (formic acid), temperature, structural parameters such as η^6-coordinated arene and the N–H bonds in the ethylenediamine-based ligands, on the catalytic transformation of furfural to LA were investigated.

Initial results indicated that complete conversion of furfural (**1a**) to LA (**2a**) with >99% selectivity was achieved with 5 mol% of **[Ru]-1** in the presence of 12 equivalents of formic acid after reaction for 24 h at 80 °C. Analysis of the product by ^{1}H NMR spectroscopy (δ = 2.73 (t, $-CH_2$, C2), 2.60 (t, $-CH_2$, C3), and 2.17 ppm (s, $-CH_3$, C5)), ^{13}C NMR and HRMS analysis further confirmed the formation of LA (*m/z* found = 139.0365 [$C_5H_8O_3$+Na^+] and *m/z* calculated = 139.0366 [$C_5H_8O_3$+Na^+]) (Figure 2). These results, indeed, indicate the decisive role of the **[Ru]-1** catalyst, with a positive cooperation from formic acid, for the tandem catalytic transformation of furfural with high selectivity to LA.

Further, the reaction completion time was fine-tuned by optimizing the reaction temperature (Figure 3(a)). Decreasing the reaction temperature to 60 °C resulted in a significant loss of the catalytic activity, and at 40 °C catalytic reaction was stopped. However, reactions performed at 100 °C displayed complete conversion of furfural to LA in a shorter reaction time (8 h). To further optimize the formic acid amount, reactions were performed with the formic acid amount ranging from 0 to 24 equivalents (Figure 3(b)). Complete conversion of furfural with >99% selectivity for LA was achieved in the presence of ≥12 equivalents of formic acid, whereas decreasing the formic acid amount below 12 equivalents resulted a decrease in conversion of furfural and the selectivity for LA was

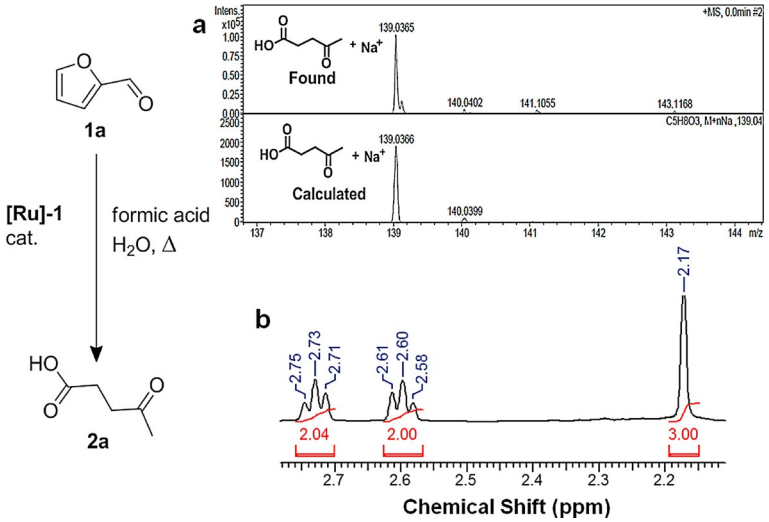

Figure 2. Catalytic transformation of furfural to LA in the presence of **[Ru]-1** catalyst and formic acid in water, and the identification of LA by (a) HRMS and (b) ^{1}H NMR spectroscopy.

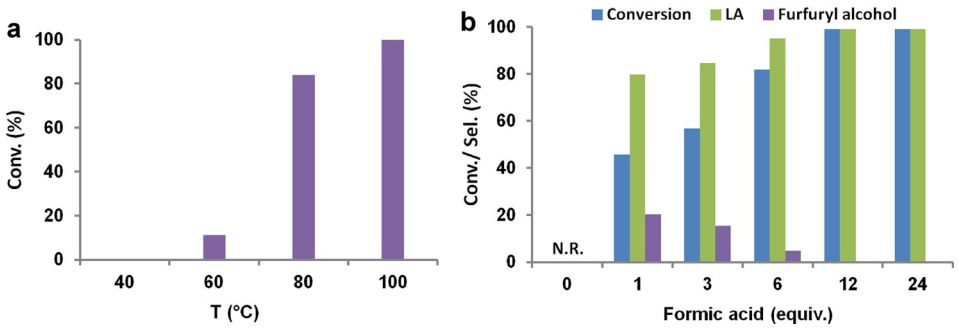

Figure 3. Effect of (a) reaction temperature and (b) formic acid concentration on the catalytic transformation of furfural to LA in the presence of **[Ru]-1** in water. Reaction conditions: (a) furfural (1.0 mmol), catalyst (5 mol%), formic acid (12 equiv.), and water (10 mL) at different temperatures for 8 h. (b) Furfural (1.0 mmol), catalyst (5 mol%), formic acid (as specified), and water (10 mL) at 100 °C for 8 h.

also compromised. Interestingly, for the catalytic reaction with lower formic acid amounts, the hydrogenated intermediate, furfuryl alcohol, was also observed along with the LA. Moreover, it is worth mentioning that no conversion of furfural was observed for the catalytic reaction performed in the absence of formic acid (Figure 3(b) and Figure S1 in the Supporting Information). Interestingly, when furfural was treated with formic acid, in the absence of the catalyst, only humin formation was observed (Figure S1).[20] Furthermore, replacement of formic acid with short-chain or bulky acids such as acetic acid, propionic acid, or *iso*-butyric acid also resulted in no conversion of furfural (Table S3 in the Supporting Information). As the formation of metal–hydride bond, a crucial step in the transfer hydrogenation reaction, is only possible in the presence of formic acid, other acids could not contribute to the metal-catalyzed transfer hydrogenation for the transformation of furfural to furfuryl alcohol, and therefore resulted in no reaction. Further evidence to support the dual role of the formic acid during the catalytic reaction was gained by performing the transformation of furfural in the presence of **[Ru]-1** catalyst and replacing formic acid with hydrogen gas under optimized reaction conditions. Contrary to the high activity achieved in the presence of formic acid, replacing formic acid with hydrogen gas resulted in no conversion of furfural. These observations strongly support the significant role of formic acid for the tandem catalytic transformation of furfural to levulinic acid via furfuryl alcohol, where the crucial transfer hydrogenation step can only take place in the presence of formic acid, but not with other organic acids or hydrogen gas under our optimized reaction conditions.

Having optimized the reaction conditions, the influence of the other arene–Ru^{II} catalysts, **[Ru]-2**–**[Ru]-8**, containing either varying ethylenediamine derivatives or η^6-arene ligands, on the catalytic transformation of furfural to LA was investigated. As depicted in Figure 4, of the various ethylenediamine ligands used, the ruthenium catalysts **[Ru]-1** and **[Ru]-5**, with unsubstituted ethylenediamine, performed the best. The catalytic activity was in the order of **[Ru]-1** > **[Ru]-2** > **[Ru]-3** > **[Ru]-4**, which clearly indicates the significant role of the N–H bond in the enhanced catalytic activity of the **[Ru]-1** catalyst. Moreover, a close analogue of the highly active **[Ru]-1** catalyst, an analog that contains the *N*-tosylated ethylenediamine (Ts-en) ligand in

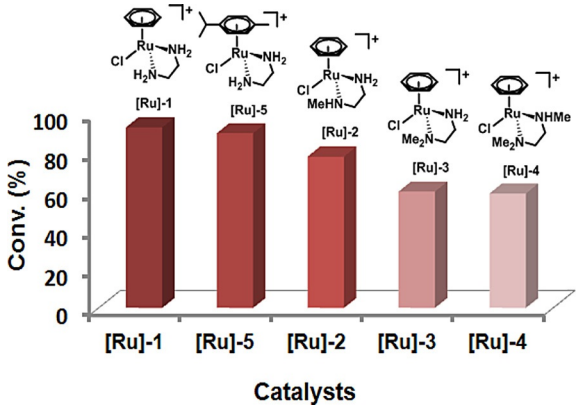

Figure 4. Catalytic transformation of furfural to LA by arene–Ru^{II} complexes in water. Reaction conditions: furfural (1.0 mmol), catalyst (5 mol%), formic acid (12 equiv.), and water (10 mL) at 100 °C for 8 h.

place of ethylenediamine, was found to be only slightly less active than the **[Ru]-1** catalyst. Although the Ru-*p*-cymene catalyst (**[Ru]-5**) was found to be slightly less active than its close analogue, Ru-benzene catalyst (**[Ru]-1**), an analogous trend in the catalytic activity was also observed with the change in the N–H entities for the catalysts **[Ru]-6**–**[Ru]-8** (Figure S2 in the Supporting Information).

These observations indicated a significant structure–activity relationship driving the catalytic activity of the studied arene–Ru^{II} complexes. The role of N–H bonds present in the ruthenium complexes during the transfer hydrogenation process is well established.[24] The mechanistic study of the catalytic transformation of furfural inferred an initial transfer hydrogenation of furfural to furfuryl alcohol, which subsequently undergoes formic acid assisted hydrolytic ring opening to levulinic acid. We strongly believe that, in our case, N–H bonds also play a significant role in controlling the catalytic activity of the studied ruthenium complexes, particularly for the initial transformation of furfural to furfuryl alcohol, and therefore **[Ru]-1**, with a high availability of N–H bonds, showed the highest catalytic activity. Moreover, the higher activity of the benzene complex over *p*-cymene complex was presumably due to the combined steric and electronic effect of the arene ligands.[24] Thus, all the further optimizations and explorations of the cata-

lytic transformation reactions of furan derivatives was done using the highly active ruthenium catalyst **[Ru]-1**.

To further investigate the progress of the catalytic reaction and to identify any possible intermediate components (possibly hydrogenated products), UV/Vis and ^{1}H NMR spectra were collected as a function of time for the catalytic transformation of furfural to LA in the presence of **[Ru]-1**, in water at 100 °C (Figures 5 and 6). With increasing reaction time, a gradual decrease was observed in the intensity of the absorption band at 276 nm in the UV/Vis spectra, which corresponds to furfural (Figure 5). Although the band from LA was not distinguishable, the observed UV/Vis pattern indicated that furfural was being used up during the course of the reaction. The kinetic plot (Figure 5, inset) of the catalytic reaction, based on the absorbance values at 276 nm for the initial 8 h, showed a linear correlation between $\ln(C_t/C_0)$ and reaction time, which suggests that the reaction follows pseudo-first-order kinetics ($k = 5.67 \times 10^{-5}$ s^{-1}). A series of reactions for the catalytic transformation of furfural was further carried out by using a fixed initial concentration (1.2 mol L^{-1}) of formic acid while varying the concentration of furfural (0.05 to 0.15 mol L^{-1}). The initial rates indicated that the catalytic reaction follows first-order kinetics with furfural concentration (Figure S3 in the Supporting Information). Moreover, the kinetic study performed by using a fixed concentration of furfural (0.10 mol L^{-1}) with varying formic acid concentrations (0.6 to 2.4 mol L^{-1}) indicated that, contrary to the trends observed with furfural concentration, the reaction rate was not sensitive to the concentration of formic acid (Table S4 in the Supporting Information).

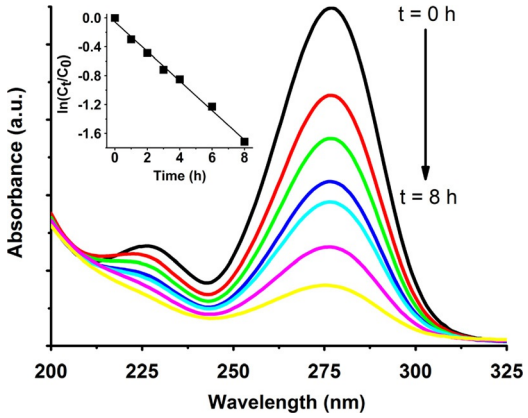

Figure 5. UV/Vis spectra as a function of time for the catalytic transformation of furfural to LA in water. Inset: kinetic profile for the initial 8 h at 276 nm. Reactions were performed by using 5 mol% arene–Ru^{II} catalyst **[Ru]-1** in the presence of formic acid (12 equiv.) at 100 °C.

Time-resolved ^{1}H NMR spectra were recorded to monitor the progress of the **[Ru]-1**-catalyzed transformation of furfural over a period of 12 h. We observed that the intensities of the resonances resulting from LA at $\delta = 2.73$ (t, $-CH_2$, C2), 2.60 (t, $-CH_2$, C3), and 2.17 ppm (s, $-CH_3$, C5) increase with the progress of the catalytic reaction (Figure 6). The reaction profiles with respect to time, shown in Figure 6(b), depict that, in the initial hours of the catalytic reaction, there is formation of the hydrogenated intermediate, furfuryl alcohol; however, this intermediate soon disappeared with the progress of the catalytic reaction and LA appeared as the only major product. These results are in accordance with previous reports, where in the reaction performed employing furfuryl alcohol, instead of furfural, its facile transformation to LA was comfortably achieved even in the absence of catalyst.[17] The assumption that the intermediate, furfuryl alcohol, presumably undergoes facile ring opening in the presence of formic acid, was further supported by the appearance of furfuryl alcohol in the reactions performed with lower amounts (< 12 equivalents) of formic acid. However, furfuryl alcohol soon disappeared with increased formic acid amounts. These important observations and the isolation of the intermediate, furfuryl alcohol, inferred that, presumably, the **[Ru]-1** catalyst initially catalyzed the hydrogenation of furfural to the corresponding furfuryl alcohol by transfer hydrogenation by using formic acid as the hydrogen source, and later the furfuryl alcohol instantly undergoes ring opening to LA by an acid-promoted hydrolysis to achieve the tandem catalytic transformation of furfural to levulinic acid, as exemplified in Figure S4 (in the Supporting Information).[16,17]

To further investigate the generality of the **[Ru]-1** catalyst, catalytic transformations of other furan derivatives with differ-

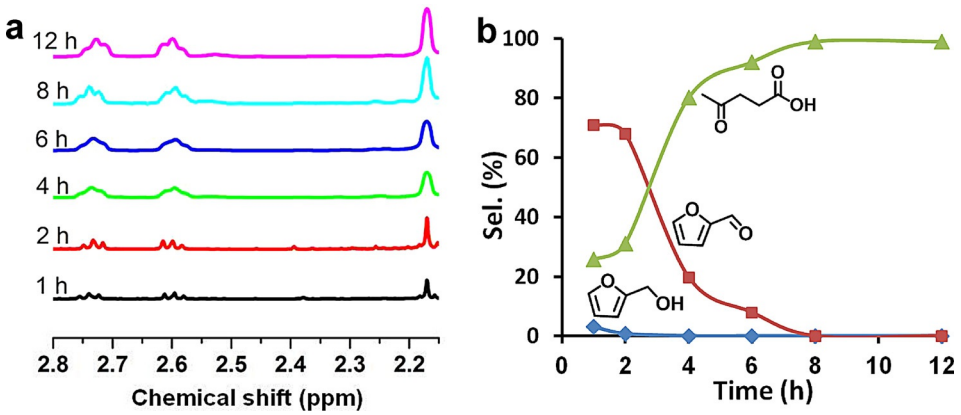

Figure 6. (a) Time-resolved ^{1}H NMR spectra and (b) corresponding reaction profiles for the catalytic transformation of furfural to LA in water by using 5 mol% **[Ru]-1** catalyst in the presence of formic acid (12 equiv.) at 100 °C.

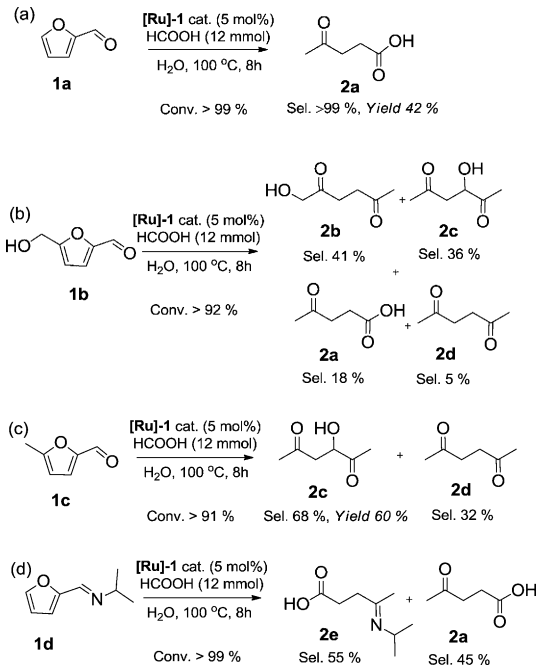

Scheme 2. Catalytic transformation of furan by **[Ru]-1** in water.

ent substituents at the 2 and 5 positions, such as 5-HMF (**1b**), 5-MF (**1c**), and *N*-(furan-2-ylmethylene)propan-2-amine (**1d**), were investigated under the optimized reaction conditions (5 mol% **[Ru]-1**, 12 equiv. formic acid, 100 °C, 8 h) (Scheme 2). Complete conversion of furfural with >99% selectivity to LA (isolated yield 42%) was achieved in 8 h (Scheme 2(a)). Under identical reaction conditions, 92% conversion of 5-HMF was achieved, where 1-hydroxyhexane-2,5-dione (1-HHD, **2b**), 3-HHD (**2c**), LA (**2a**), and hexane-2,5-dione (2,5-HD; **2d**) were observed as the products with selectivities of 41, 36, 18, and 5%, respectively (Scheme 2(b)). Conversion of 5-HMF to 1-HHD also occurred in accordance with previous reports, where it was reported as one of the major products when using catalytic systems based on Pd/C, Cp*–Ir complexes, or arene–Ru^{II} catalysts.[15–17] Reaction with 5-MF (**1c**) yielded 60% 3-HHD (**2c**), where the relative selectivity for 3-HHD and 2,5-HD were 68 and 32%, respectively (Scheme 2(c)). Moreover, the reaction was also performed with *N*-(furan-2-ylmethylene)propan-2-amine (**1d**), obtained by the condensation of furfural with isopropylamine. Interestingly, the reaction products obtained were LA and isopropylamine-condensed LA (*N*-(isopropylimino)pentanoic acid, **2e**) in approximately 1:1 molar ratio (Scheme 2(d)). The formation of the product **2e** indicated that, presumably, the imine bond in the substrate **1d** hydrolyzed during the catalytic reaction and later condensed with the ketonic group of the LA to yield **2e**.

Catalyst stability, recovery, and recycling

The thermal stability of the ruthenium catalyst **[Ru]-1** was studied by performing ^{1}H NMR experiments and thermal gravimetric analysis (TGA) measurements. The decomposition of the catalyst was monitored at certain intervals of time (0–72 h) by ^{1}H NMR spectroscopy, where no evidence of decomposition was observed (Figure S5 in the Supporting Information). Moreover, the TGA graphs clearly indicated that **[Ru]-1** catalyst is stable up to 200 °C (Figure S6 in the Supporting Information). Further, mercury poisoning experiments showed no significant change in the catalytic activity of **[Ru]-1** catalyst in the presence of an excess of Hg^0, which strongly indicates the homogenous nature of the catalyst. Although the homogeneous nature of the catalyst provides several advantages, the easy recovery of catalysts of homogeneous catalytic reactions remains an inherent limitation. However, we are fortunate that the high aqueous solubility of the **[Ru]-1** catalyst gave us an opportunity for easy recovery of the catalyst and its reuse for further catalytic cycles for the transformation of furfural to LA. After each catalytic run, reaction mixture was extracted by using a suitable organic solvent, while the catalyst, which remains in the aqueous phase, was immediately used for the next catalytic run by adding additional specified amounts of the furfural and formic acid. The **[Ru]-1** catalyst was recycled for at least five consecutive catalytic cycles, without significant loss of the catalytic activity (Figure 7).

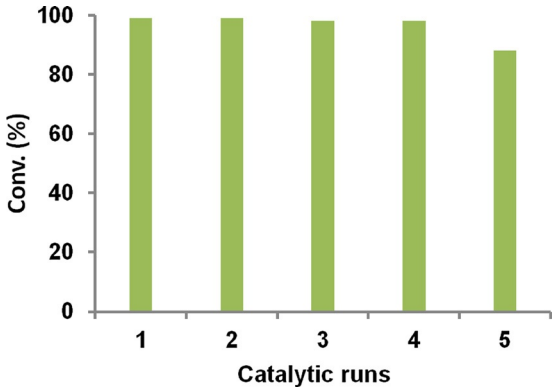

Figure 7. Recyclability of **[Ru]-1** catalyst for the catalytic transformation of furfural to LA in the presence of formic acid (12 equiv.) in water at 100 °C.

These results further demonstrated the high stability of the **[Ru]-1** catalyst in water. Moreover, scanning electron microscopic (SEM) images (Figure S7 in the Supporting Information) of the fresh catalyst and the catalyst recovered after the catalytic reaction showed no remarkable morphological changes of the **[Ru]-1** catalyst during the reaction. These observations were further authenticated by the presence of peaks corresponding to the protons and carbon atoms of the ethylenediamine and arene ligands in the NMR spectra of the **[Ru]-1** catalyst recovered after the catalytic reactions (Figure S8 in the Supporting Information), peaks that are consistent with the those of the fresh **[Ru]-1** catalyst. Moreover, ESI mass spectral data of the catalyst recovered after the catalytic reaction was also found to be analogous to that of the fresh catalyst (Figure S9 in the Supporting Information). The above analyses ensure that there is no significant deformation in the catalyst structure, which is consistent with the observed high catalytic

recyclability, up to five consecutive catalytic runs, for the catalyst in the studied catalytic transformation.

Catalytic transformation of fructose to LA and diketones

Next, we explored the catalytic transformation of fructose to LA and diketones in the presence of 5 mol% **[Ru]-1** catalyst (Scheme 3).

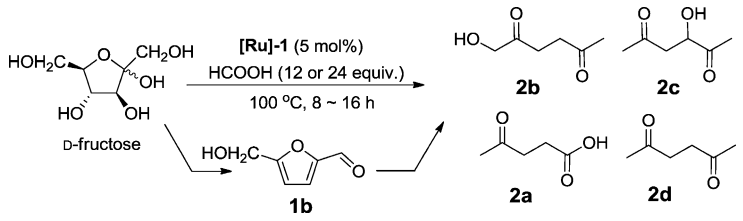

Scheme 3. Catalytic transformation of fructose to LA and diketones.

After heating fructose at 100 °C for 8 h in the presence of 12 equivalents of formic acid, conversion of fructose to 1-HHD and LA as the major products were achieved with 27 and 51% selectivity, respectively, along with 5-HMF (5%), diketone (4%), and 3-HHD (13%) as minor products. The reaction products obtained from fructose transformation were found to be analogous to the products obtained with 5-HMF, suggesting that, presumably, the reaction proceeds through the initial formation of 5-HMF.[3] Moreover, by increasing the reaction time to 16 h or doubling the formic acid amount (24 equiv.), the selectivity for 1-HHD increased and 87% selectivity was observed when the reaction was performed at 100 °C for 16 h in the presence of 12 equivalents of formic acid. Unfortunately, attempts to use glucose in place to fructose failed, possibly because the **[Ru]-1** catalyst cannot catalyze the isomerization of glucose to fructose. Despite the low fructose transformation observed for the catalytic reaction, it is worth noting that the direct catalytic transformation of fructose to open-ring components such as LA and diketones can also be achieved with ruthenium-based homogenous catalysts.

Most of the studies on the transformation of furans have been performed in autoclaves by using mineral acids or H_2 gas with high pressure and temperature.[15,16,25–28] Among these, there are many reports on the catalytic transformation of 5-HMF to ketoacids and diketones, particularly by using heterogeneous catalysts, whereas studies with homogeneous catalyst are relatively few.[14,15b,16,17,25–30] Li et al. employed Amberlyst 70 for furfural transformation in water, as well as methanol, and observed that furfural converted to a polymer in both reaction media.[15a] Even by using Pd/Al_2O_3 with Amberlyst 70 and 70 bar H_2 at 165 °C in methanol, only low yields (23.1 and 2.4%) of methyl-levulinate and levulinic acid were achieved, whereas Pd/Al_2O_3 on its own was found to be inactive.[26] Riisager et al. explored $Ru(OH)_x/Al_2O_3$ catalysts for the aerobic oxidation of 5-HMF at 140 °C, where LA was observed as a side product along with the oxygenated products 2,5-furandicarboxylic acid and so on.[30] Also, LA was observed as a by-product during the catalytic hydrogenation of furfural and 5-HMF over a $Pd–Ir/SiO_2$ catalyst.[27] In the transformation of furans, catalysts are generally active at higher temperatures [Pd/C (120 °C), Au/Nb_2O_5 (140 °C), Pd/Al_2O_3 (140 °C), $Ni–Al_2O_3$ (180 °C)].[14,15b,28,29] Catalytic transformations with homogeneous catalysts show narrow product distributions and greater selectivity towards the open-ring products, for instance, with Cp*–Ir catalysts and arene–Ru^{II} catalysts.[16,17] Moreover, ruthenium-based homogeneous catalysts were found to be highly active and recyclable even in aqueous media.[17] In the present study, arene–Ru complexes containing ethylenediamine ligands were also found to be highly active and stable even at 100 °C in water and open atmospheric conditions, and can be recycled in up to five consecutive catalytic cycles without any significant loss in the catalytic activity. Moreover, the studied arene–Ru catalyst **[Ru]-1** has shown potential to convert fructose to LA and diketones (1-HHD, 3-HHD, 2,5-HD) in water under moderate reaction conditions.

Conclusions

Highly active water-soluble homogenous catalysts based on arene–ruthenium(II) complexes containing simple and readily available ethylenediamine (or its derivatives) ligands, were successfully employed for the catalytic transformation of bio-derived furans into open-ring value-added ketoacid (LA) and diketones (1-HHD, 3-HHD, and 2,5-HD) in the presence of formic acid. Depending upon the furan used, formic acid concentration, reaction temperature, and the catalyst, catalytic conversion, selectivity, and the product distribution can be fine-tuned. The N–H bonds present in the ruthenium catalyst were shown to exert a significant on the catalytic transformation, where the most active catalyst has the highest number of N–H bonds. Moreover, direct catalytic transformation of fructose to 1-HHD and LA was also achieved with limited conversion. Mechanistic studies involving ^1H NMR spectroscopy and experiments with variable formic acid concentrations revealed a tandem mode of catalytic transformation of furfural to LA via the hydrogenated intermediate, furfuryl alcohol. Furthermore, high aqueous solubility and stability of the ruthenium catalyst offers the potential for easy recovery and reusability in at least five consecutive catalytic runs without any significant loss of the catalytic activity. Through our study, we have demonstrated a significant cooperation between the ruthenium catalyst and formic acid to achieve high catalytic turnover for the transformation of furans. We believe that this work will encourage extensive research on the design and development of simple yet active catalysts for this or several other important catalytic transformations in the fine chemical industry and biofuel-based energy sector.

Experimental Section

Materials and methods

All reactions were performed without inert gas protection, using chemicals of high purity purchased from Aldrich or Alfa Aesar. Dichloro-bridged arene–Ru^{II} precursors $[\{(\eta^6\text{-}C_6H_6)RuCl_2\}_2]$ and $[\{(\eta^6\text{-}$

$C_{10}H_{14})RuCl_2\}_2$] were synthesized according to the literature procedures.[31] The catalytic reactions were monitored by using a thin layer chromatography (TLC). ^{1}H NMR (400 MHz), ^{13}C NMR (100 MHz), and ^{31}P NMR (161.97 MHz) spectra were recorded at 298 K by using $CDCl_3$, D_2O, or [D_6]DMSO as the solvent on a Bruker Avance 400 spectrometer. Tetramethylsilane (TMS) was used as an external standard and the chemical shifts in ppm are reported relative to the center of the singlet at 7.26 ppm for $CDCl_3$, 4.75 for D_2O, and 2.49 ppm for [D_6]DMSO in ^{1}H NMR spectra and to the center of the triplet at 77.0 ppm for $CDCl_3$ and 39.50 ppm for [D_6]DMSO in ^{13}C NMR spectra. Suitable single crystals of the arene–Ru^{II} complexes **[Ru]-2**, **[Ru]-6**, **[Ru]-7**, and **[Ru]-8** were subjected to single-crystal X-ray structural studies by using an Agilent Technologies Supernova CCD system. ESI (positive and negative mode) and high-resolution mass spectra (HRMS) were recorded on a micro TF-Q II mass spectrometer. UV/Vis spectra were performed on a Varian Cary 100 Bio UV/Vis spectrophotometer and a Shimadzu UV-1700 PharmaSpec UV/Vis spectrophotometer using 10 mm quartz cuvettes. To study the kinetics of the catalytic reactions by UV/Vis spectrophotometry, a small portion of the reaction mixture (100 μL), taken at different time intervals, was added to distilled water (3 mL) and the spectra were obtained. To calculate the rate constant of the catalytic reaction, the ratio of C_t and C_0, where C_t is the concentration at time 't' and C_0 is the initial concentration, was measured by using the relative intensity ratio of the respective absorbance A_t/A_0 at 276 nm. GC-MS analysis was performed on a PerkinElmers GC gas chromatograph Clarus 680 coupled with a PerkinElmers mass spectrometer Clarus SQ8T in the EI (Electron Impact) mode and using a capillary column ELITE 5 (30 m × 0.25 mm). Thermal gravimetric analyses (TGA) were performed on the Mettler Toledo thermal analysis system. Scanning electron microscopy (SEM) images and elemental mapping data were collected on a Carl Zeiss supra 55 (operating voltage 15 kV), by using amorphous carbon-coated 400 mesh copper grids for the deposited sample.

Synthesis of ruthenium catalysts ([Ru]-1–[Ru]-8)

Arene–Ru^{II} complexes **[Ru]-1**–**[Ru]-8** were synthesized by using a modified literature method.[22] A methanol solution (25 mL) of the dichloro-bridged arene–Ru^{II} dimer (0.2 mmol) and the suitable ethylenediamine or *N*-substituted ethylenediamine (0.4 mmol) was stirred at room temperature (298 K) for 3 h, filtered, and NH_4PF_6 (1.0 mmol) was added to the filtrate. The total volume of the solution was slowly reduced to approximately 10 mL on a rotary evaporator and, after cooling overnight at 4 °C, the microcrystalline product was obtained, which was collected by filtration, washed with ether, and recrystallized from methanol/CH_2Cl_2/ether.

Catalytic reaction for the conversion of furans/fructose to LA/diketones

Furan/fructose (1.0 mmol) and formic acid (as specified) were added to an aqueous suspension (10 mL) of arene–Ru^{II} catalyst (5 mol%), and the reaction mixture was stirred for a specified time at 100 °C (oil bath). After the catalytic reaction was complete, the reaction mixture was extracted with ethylacetate (4 × 10 mL), the organic extract was washed with brine (5 mL), and dried with Na_2SO_4. The solvent was removed in vacuo. The obtained products were separated by column chromatography on silica gel with *n*-hexane/ethylacetate (98:2 to 90:10) as the eluents. The product 3-hydroxyhexane-2,5-dione (3-HHD) obtained from the catalytic transformation of 5-methylfurfural (5-MF) was separated and purified by column chromatography on silica gel with a 10% ethylacetate/hexane mixture (400 mL). Then, the product was isolated by removing the solvent in vacuo. The product levulinic acid (LA) was obtained by adding saturated sodium bicarbonate solution to the organic extract (reduced volume to ca. 5 mL) until effervescence ceases. Then, the mixture was washed with ethylacetate (4 × 10 mL). The combined water portion was neutralized with dilute hydrochloric acid, and the product was extracted with ethylacetate (4 × 10 mL). LA was isolated by removing the solvent in vacuo. During the extraction, separation, and purification processes, the organic and aqueous portions were continuously monitored by thin layer chromatography (TLC) under a UV chamber or by staining with iodine. The reaction products were identified by ^{1}H NMR, ^{13}C NMR, HRMS, and GCMS analysis. Conversions and selectivities were determined by ^{1}H NMR spectroscopy. Isolated yields were determined from the products obtained from the purification process as described above.

Acknowledgments

The authors thank IIT Indore, CSIR, New Delhi, and SERB (DST), New Delhi, for financial support. SIC, IIT Indore is acknowledged for use of its instrumental facilities. Sincere thanks go to Prof. Pratibha Sharma, DAVV, Indore, for her help in performing the kinetic study. A.D.D. thanks the CSIR New Delhi research scheme (01(2722)/13/EMR-II) for a JRF grant. K.G. and R.K.R. thank CSIR New Delhi for their SRF grants. D.T. thanks UGC New Delhi for a SRF grant.

Keywords: diketones · furans · levulinic acid · tandem catalysis · water

[1] a) D. L. Klass, *Biomass for Renewable Energy, Fuels, and Chemicals*, Academic Press, San Diego, **1998**; b) R. A. Sheldon, *Green Chem.* **2014**, *16*, 950–963; c) M. J. Climent, A. Corma, S. Iborra, *Green Chem.* **2014**, *16*, 516–547; d) L. Hu, G. Zhao, W. Hao, X. Tang, Y. Sun, L. Lin, S. Liu, *RSC Adv.* **2012**, *2*, 11184–11206; e) S. Van de Vyver, J. Geboers, P. A. Jacobs, B. F. Sels, *ChemCatChem* **2011**, *3*, 82–94; f) A. Corma, S. Iborra, A. Velty, *Chem. Rev.* **2007**, *107*, 2411–2502; g) L. Petrus, M. A. Noordermeer, *Green Chem.* **2006**, *8*, 861–867; h) G. W. Huber, J. N. Chheda, C. J. Barrett, J. A. Dumesic, *Science* **2005**, *308*, 1446–1450.

[2] a) A. M. Ruppert, K. Weinberg, R. Palkovits, *Angew. Chem. Int. Ed.* **2012**, *51*, 2564–2601; *Angew. Chem.* **2012**, *124*, 2614–2654; b) R. Xing, A. V. Subrahmanyam, H. Olcay, W. Qi, G. P. van Walsum, H. Pendse, G. W. Huber, *Green Chem.* **2010**, *12*, 1933–1946.

[3] a) K. Tajvidi, P. J. C. Hausoul, R. Palkovits, *ChemSusChem* **2014**, *7*, 1311–1317; b) A. Yepez, A. Garcia, M. S. Climent, A. A. Romero, R. Luque, *Catal. Sci. Technol.* **2014**, *4*, 428–434; c) R. Alamillo, A. J. Crisci, J. M. R. Gallo, S. L. Scott, J. A. Dumesic, *Angew. Chem. Int. Ed.* **2013**, *52*, 10349–10351; *Angew. Chem.* **2013**, *125*, 10539–10541; d) A. Yepez, A. Pineda, A. Garcia, A. A. Romero, R. Luque, *Phys. Chem. Chem. Phys.* **2013**, *15*, 12165–12172; e) H. Kimura, M. Nakahara, N. Matubayasi, *J. Phys. Chem. A* **2013**, *117*, 2102–2113; f) J. Zhang, E. Weitz, *ACS Catal.* **2012**, *2*, 1211–1218; g) T. Thananatthanachon, T. B. Rauchfuss, *ChemSusChem* **2010**, *3*, 1139–1141.

[4] a) X. Yi, I. Delidovich, Z. Sun, S. Wang, X. Wang, R. Palkovits, *Catal. Sci. Technol.* **2015**, *5*, 2496–2502; b) N. A. S. Ramli, N. A. S. Amin, *J. Mol. Catal. A* **2015**, *407*, 113–121; c) H. Huang, C. A. Denard, R. Alamillo, A. J. Crisci, Y. Miao, J. A. Dumesic, S. L. Scott, H. Zhao, *ACS Catal.* **2014**, *4*, 2165–2168; d) L. Wu, J. Song, B. Zhang, B. Zhou, H. Zhou, H. Fan, Y. Yang, B. Han, *Green Chem.* **2014**, *16*, 3935–3941; e) J. Song, H. Fan, J. Ma, B. Han, *Green Chem.* **2013**, *15*, 2619–2635; f) F. H. Richter, K. Pupovac, R. Palkovits, F. Schüth, *ACS Catal.* **2013**, *3*, 123–127; g) A. J. Crisci, M. H. Tucker, M.-Y. Lee, S. G. Jang, J. A. Dumesic, S. L. Scott, *ACS Catal.*

2011, *1*, 719 – 728; h) S. Hu, Z. Zhang, J. Song, Y. Zhou, B. Han, *Green Chem.* **2009**, *11*, 1746 – 1749.

[5] a) R. J. van Putten, J. C. van der Waal, E. de Jong, C. B. Rasrendra, H. J. Heeres, J. G. de Vries, *Chem. Rev.* **2013**, *113*, 1499 – 1597; b) Y. Nakagawa, M. Tamura, K. Tomishige, *ACS Catal.* **2013**, *3*, 2655 – 2668; c) J. C. Serrano-Ruiz, R. Luque, A. Sepulveda-Escribano, *Chem. Soc. Rev.* **2011**, *40*, 5266 – 5281.

[6] a) S. Liu, Y. Amada, M. Tamura, Y. Nakagawa, K. Tomishige, *Green Chem.* **2014**, *16*, 617 – 626; b) Y. Yang, Z. Du, Y. Huang, F. Lu, F. Wang, J. Gao, J. Xu, *Green Chem.* **2013**, *15*, 1932 – 1940; c) J. Chen, F. Lu, J. Zhang, W. Yu, F. Wang, J. Gao, J. Xu, *ChemCatChem* **2013**, *5*, 2822 – 2826; d) Y. Nakagawa, H. Nakazawa, H. Watanabe, K. Tomishige, *ChemCatChem* **2012**, *4*, 1791 – 1797; e) W. Xu, H. Wang, X. Liu, J. Ren, Y. Wang, G. Lu, *Chem. Commun.* **2011**, *47*, 3924 – 3926.

[7] a) J. Artz, S. Mallmann, R. Palkovits, *ChemSusChem* **2015**, *8*, 672 – 679; b) J. M. R. Gallo, D. M. Alonso, M. A. Mellmer, J. A. Dumesic, *Green Chem.* **2013**, *15*, 85 – 90; c) F. L. Grasset, B. Katryniok, S. Paul, V. Nardello-Rataj, M. Pera-Titus, J.-M. Clacens, F. D. Campo, F. Dumeignil, *RSC Adv.* **2013**, *3*, 9942 – 9948; d) T. Pasini, M. Piccinini, M. Blosi, R. Bonelli, S. Albonetti, N. Dimitratos, J. A. Lopez-Sanchez, M. Sankar, Q. He, C. J. Kiely, G. J. Hutchings, F. Cavani, *Green Chem.* **2011**, *13*, 2091 – 2099; e) S. E. Davis, L. R. Houk, E. C. Tamargo, A. K. Datye, R. J. Davis, *Catal. Today* **2011**, *160*, 55 – 60.

[8] a) Q.-N. Xia, Q. Cuan, X.-H. Liu, X.-Q. Gong, G.-Z. Lu, Y.-Q. Wang, *Angew. Chem. Int. Ed.* **2014**, *53*, 9755 – 9760; *Angew. Chem.* **2014**, *126*, 9913 – 9918; b) M. Li, X. Xu, Y. Gong, Z. Wei, Z. Hou, H. Li, Y. Wang, *Green Chem.* **2014**, *16*, 4371 – 4377; c) G. Li, N. Li, S. Li, A. Wang, Y. Cong, X. Wang, T. Zhang, *Chem. Commun.* **2013**, *49*, 5727 – 5729; d) A. D. Sutton, F. D. Waldie, R. Wu, M. Schlaf, L. A. P. Silks, III, J. C. Gordon, *Nat. Chem.* **2013**, *5*, 428 – 432; e) S. Sitthisa, D. E. Resasco, *Catal. Lett.* **2011**, *141*, 784 – 791; f) Z. Xinghua, W. Tiejun, M. Longlong, W. Chuangzhi, *Fuel* **2010**, *89*, 2697 – 2702.

[9] D. G. Alberg, T. B. Poulsen, S. Bertelsen, K. L. Christensen, R. D. Birkler, M. Johannsen, K. A. Jørgensen, *Bioorg. Med. Chem. Lett.* **2009**, *19*, 3888 – 3891.

[10] J. Zhang, S. B. Wu, B. Li, H. D. Zhang, *ChemCatChem* **2012**, *4*, 1230 – 1237.

[11] J. J. Bozell, G. R. Petersen, *Green Chem.* **2010**, *12*, 539 – 554.

[12] a) J. Song, L. Wu, B. Zhou, H. Zhou, H. Fan, Y. Yang, Q. Meng, B. Han, *Green Chem.* **2015**, *17*, 1626 – 1632; b) A. Phanopoulos, A. J. P. White, N. J. Long, P. W. Miller, *ACS Catal.* **2015**, *5*, 2500 – 2512; c) X. Tang, X. Zeng, Z. Li, W. Li, Y. Jiang, L. Hu, S. Liu, Y. Sun, L. Lin, *ChemCatChem* **2015**, *7*, 1372 – 1379; d) J. Tan, J. Cui, T. Deng, X. Cui, G. Ding, Y. Zhu, Y. Li, *ChemCatChem* **2015**, *7*, 508 – 512; e) X. Tang, Z. Li, X. Zeng, Y. Jiang, S. Liu, T. Lei, Y. Sun, L. Lin, *ChemSusChem* **2015**, *8*, 1601 – 1607; f) I. Podolean, V. Kuncser, N. Gheorghe, D. Macovei, V. I. Parvulescu, S. M. Coman, *Green Chem.* **2013**, *15*, 3077 – 3082; g) W. R. H. Wright, R. Palkovits, *ChemSusChem* **2012**, *5*, 1657 – 1667; h) G. Berkovitch, D. Doron, A. Nudelman, Z. Malik, A. Rephaeli, *J. Med. Chem.* **2008**, *51*, 7356 – 7369; i) R. Vallinayagam, F. Schmitt, J. Barge, G. Wagnieres, V. Wenger, R. Neier, L. Juillerat-Jeanneret, *Bioconjugate Chem.* **2008**, *19*, 821 – 839.

[13] M. Sankar, N. Dimitratos, P. J. Miedziak, P. P. Wells, C. J. Kiely, G. J. Hutchings, *Chem. Soc. Rev.* **2012**, *41*, 8099 – 8139.

[14] J. Ohyama, R. Kanao, A. Esaki, A. Satsuma, *Chem. Commun.* **2014**, *50*, 5633 – 5636.

[15] a) X. Hu, R. J. M. Westerhof, L. Wu, D. Dong, C.-Z. Li, *Green Chem.* **2015**, *17*, 219 – 224; b) F. Liu, M. Audemar, K. D. O. Vigier, J.-M. Clacens, F. D. Campo, F. Jerome, *ChemSusChem* **2014**, *7*, 2089 – 2095.

[16] Z. Xu, P. Yan, W. Xu, X. Liu, Z. Xia, B. Chung, S. Jia, Z. C. Zhang, *ACS Catal.* **2015**, *5*, 788 – 792.

[17] K. Gupta, D. Tyagi, A. D. Dwivedi, S. M. Mobin, S. K. Singh, *Green Chem.* **2015**, *17*, 4618 – 4627.

[18] a) P. Kumar, R. K. Gupta, D. S. Pandey, *Chem. Soc. Rev.* **2014**, *43*, 707 – 733; b) M. C. Warner, C. P. Casey, J.-E. Bäckvall, *Top. Organomet. Chem.* **2011**, *37*, 85 – 125; c) B. L. Conley, M. K. Pennington-Boggio, E. Boz, T. J. Williams, *Chem. Rev.* **2010**, *110*, 2294 – 2312; d) R. Karvembu, R. Prabhakaran, K. Natarajan, *Coord. Chem. Rev.* **2005**, *249*, 911 – 918.

[19] L. H. Gong, Y.-Y. Cai, X.-H. Li, Y.-N. Zhang, J. Su, J.-S. Chen, *Green Chem.* **2014**, *16*, 3746 – 3751.

[20] a) F.-F. Wang, A.-W. Shi, X.-X. Qin, C.-L. Liu, W.-S. Dong, *Carbohydr. Res.* **2011**, *346*, 982 – 985; b) X. Hu, R. J. M. Westerhof, D. Dong, L. Wu, C.-Z. Li, *ACS Sus. Chem. Eng.* **2014**, *2*, 2562 – 2575.

[21] a) T. Pasini, G. Solinas, V. Zanotti, S. Albonetti, F. Cavani, A. Vaccari, A. Mazzanti, S. Ranieri, R. Mazzoni, *Dalton Trans.* **2014**, *43*, 10224 – 10234; b) L. Busetto, D. Fabbri, R. Mazzoni, M. Salmi, C. Torri, V. Zanotti, *Fuel* **2011**, *90*, 1197 – 1207.

[22] R. E. Morris, R. E. Aird, P. d. S. Murdoch, H. M. Chen, J. Cummings, N. D. Hughes, S. Parsons, A. Parkin, G. Boyd, D. I. Jodrell, P. J. Sadler, *J. Med. Chem.* **2001**, *44*, 3616 – 3621.

[23] a) D. Tyagi, R. K. Rai, A. D. Dwivedi, S. M. Mobin, S. K. Singh, *Inorg. Chem. Front.* **2015**, *2*, 116 – 124; b) S. K. Singh, M. Trivedi, M. Chandra, A. N. Sahay, D. S. Pandey, *Inorg. Chem.* **2004**, *43*, 8600 – 8608.

[24] A. Fujii, S. Hashiguchi, N. Uematsu, T. Ikariya, R. Noyori, *J. Am. Chem. Soc.* **1996**, *118*, 2521 – 2522.

[25] B. Girisuta, L. P. B. M. Janssen, H. J. Heeres, *Green Chem.* **2006**, *8*, 701 – 709.

[26] X. Hu, Y. Song, L. Wu, M. Gholizadeh, C.-Z. Li, *ACS Sus. Chem. Eng.* **2013**, *1*, 1593 – 1599.

[27] Y. Nakagawa, K. Takada, M. Tamura, K. Tomishige, *ACS Catal.* **2014**, *4*, 2718 – 2726.

[28] J. Tuteja, H. Choudhary, S. Nishimura, K. Ebitani, *ChemSusChem* **2014**, *7*, 96 – 100.

[29] X. Kong, R. Zheng, Y. Zhu, G. Ding, Y. Zhu, Y.-W. Li, *Green Chem.* **2015**, *17*, 2504 – 2514.

[30] Y. Y. Gorbanev, S. Kegnæs, A. Riisager, *Top. Catal.* **2011**, *54*, 1318 – 1324.

[31] a) M. A. Bennett, T. Huang, T. W. Matheson, A. K. Smith, *Inorg. Synth.* **1982**, *21*, 74 – 78; b) R. A. Zelonka, M. C. Baird, *Can. J. Chem.* **1972**, *50*, 3063 – 3072.

Received: September 13, 2015
Revised: October 9, 2015
Published online on November 23, 2015